Performance Evaluation of an Electric Vehicle Traction Drive using Si/SiC Hybrid Switches

Tan, Changyu ; Stecca, Marco; Soeiro, Thiago Batista; Dong, Jianning; Bauer, Pavol

DOI
10.1109/PEMC48073.2021.9432574

Publication date
2021

Document Version
Accepted author manuscript

Published in
Proceedings - 2021 IEEE 19th International Power Electronics and Motion Control Conference, PEMC 2021

Performance Evaluation of an Electric Vehicle Traction Drive using Si/SiC Hybrid Switches

Changyu Tan, Marco Stecca, Thiago Batista Soeiro, Jianning Dong, and Pavol Bauer
Electrical Sustainable Energy Department
Delft University of Technology, Delft 2628 CD, The Netherlands
Corresponding author: Marco Stecca, e-mail: m.stecca@tudelft.nl

***Abstract*—The parallel connection of a Silicon (Si)-based IGBT and a Silicon Carbide (SiC)-based MOSFET forming a so called hybrid switch (HyS) can be used to exploit the advantageous features of both semiconductor and materials technologies. In this paper, a HyS-based inverter designed for the application of Electric Vehicle (EV) traction is compared to the conventional inverter assembled with Si-based IGBTs and SiC-based MOSFETs. According to different standardized driving cycles, EVs operate in low partial load for a considerable amount of the time. Therefore, in this application, semiconductor conduction losses can be considerably reduced when unipolar switches such as MOSFETs are used. All in all, this work shows that the HyS configuration constitutes a good compromise between efficiency and cost when compared to the solution implementing only Si-based IGBT or solely SiC-based MOSFETs.**

***Index Terms*—Electric vehicles, hybrid switch, motor drive, Silicon Carbide (SiC), driving cycles**

I. Introduction

As the world moves towards a more sustainable future, the automotive industry aims to reduce its share of CO_2 emissions. Development of Electric Vehicles (EVs) has become prominent as they produce substantially lower CO_2 emissions than internal combustion engines vehicles [1]. One of the R&D goals in this area is the improvement of the EV traction drive efficiency and the consequent extension of driving range. The traction drive, which converts electrical energy from the battery to mechanical energy in the wheels, consists of a DC-AC converter, known as inverter, and an electric motor, as shown in Fig. 1. The inverter is a major contributor to the power loss of the traction drive [2]- [18].

Currently, the majority of the commercial EV inverters consist of Silicon (Si)-based IGBTs, which are known for robustness, relatively low cost, and good conduction performance at high currents. There are, however, several drawbacks of using Si IGBTs in the application of EV drives. Due to the bipolar junction characteristic, IGBTs have unsatisfactory performance at low current condition. Additionally, especially in high voltage class devices, the current tail observed during an IGBT's turn-off may result in high switching losses [3]. In fact, standardized driving cycles demonstrate that consumer EVs operate at low partial load during the majority of its driving [18]. This calls for a better suited semiconductor than the Si-based IGBTs.

Another candidate for the inverter switch is the Silicon Carbide (SiC) MOSFET. In recent years, it has gained popularity due to its excellent switching performance, the easy paralleling feature which can enable a higher power handling, and above all the higher temperature capability of the SiC material. The thinner n-doped region of SiC MOSFETs provide wider voltage ranges compared to the Si-based MOSFETs and have low conduction and switching losses [3]. In particular, high power SiC MOSFETs show outstanding efficiency at lower current, which makes them very suitable for application in an EV traction system from an efficiency point of view. The major drawback of the SiC MOSFET is the higher manufacturing cost and lower reliability in comparison to the traditional IGBT-based inverters.

The significantly higher cost of the SiC MOSFET calls for a compromised solution [19]. In recent years hybrid switches (HyS), assembled paralleling Si IGBT and SiC MOSFET, as shown in Fig. 2(a), have shown promising results. HySs takes advantages of both the IGBT and MOSFET technologies. Ideally at low current, the MOSFET conducts most of the current because it does not have the pn junction barrier potential. However, at high current, the IGBT branch is designed to conduct a greater proportion of the total current, due to its lower on-state resistance [3]. Furthermore, the HyS is also capable of reducing switching losses with respect to Si IGBTs. The SiC MOSFET switches faster, and thus it has considerably lower switching losses than the IGBT [9]. HyS can be controlled so to delay the turn on and off of the IGBT or to switch both IGBT and MOSFET together, as shown in Fig 2(b) and (c). Therefore, by optimizing the switching behaviour of MOSFET and IGBT in a HyS, zero voltage switching can be achieved for the IGBT to further reduce losses [9], [10], [12], [13].

Prior research has demonstrated that HyS' conduction characteristic can outperform the one of pure Si IGBTs switch

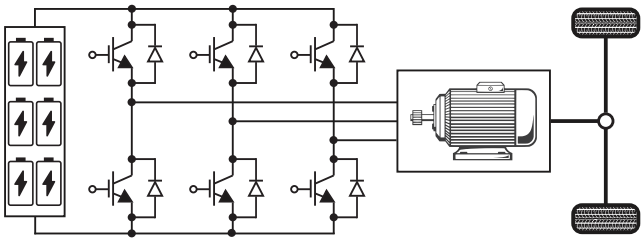

Fig. 1. Electric vehicle motor drive system with Si-based IGBT inverter.

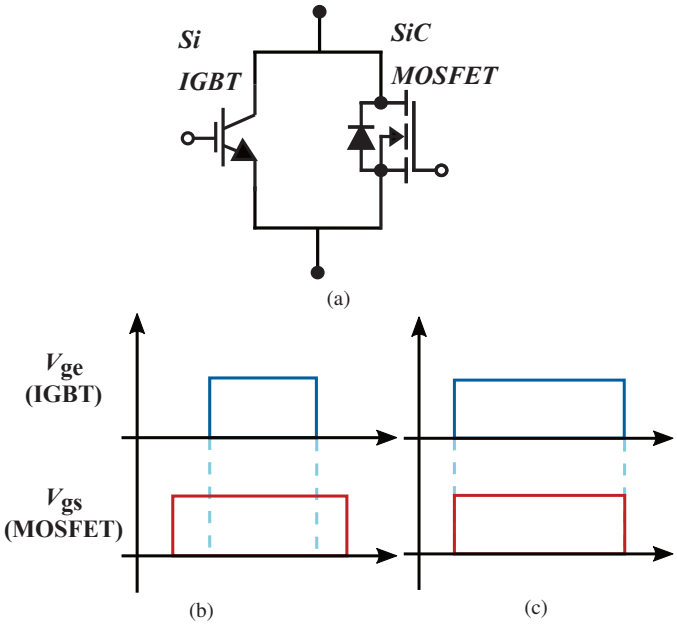

Fig. 2. Si IGBT and SiC MOSFET paralleled hybrid switch (a); gate signal for ideal switching (IGBT ZVS) (b) and for the hard switching (c).

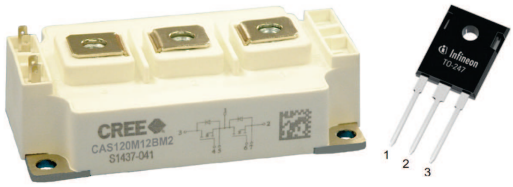

Fig. 3. Half-bridge SiC MOSFET Module [20] and Discrete Si IGBT [21].

at low current and of pure SiC MOSFETs at high current [3]. There have been some practical issues reported for the realization of the HyS, such as higher current stress and false turn-on, due to the Miller effect, across the IGBT branch [9]. However, with the appropriate control and gate driver design, these issues can be addressed with a trade-off between slightly higher losses, which still remain much lower than that of the full Si IGBT based inverter configuration [9], [11].

Several studies have already shown that HySs are a great compromise in terms of efficiency and cost between Si IGBT and SiC MOSFET. This has led the study and design of HyS-based converters in diverse applications, including in aircraft's high speed drives [16], wireless charging [15], and general high power purposes such as power modules [12]. There is a dearth of information about the HyS in the application of EV traction drives, nonetheless the peculiarity of such application might be suitable for HyS.

This paper presents a qualitative comparison of the efficiency and cost between different switch configurations of a Nissan Leaf 2011 traction inverter. A HyS-based, a full Si IGBT-based switch, and a full SiC MOSFET-based are considered. The solutions are benchmarked when performing multiple standardized driving cycles [17], [26] to evaluate the hybrid solution alongside the traditional configuration.

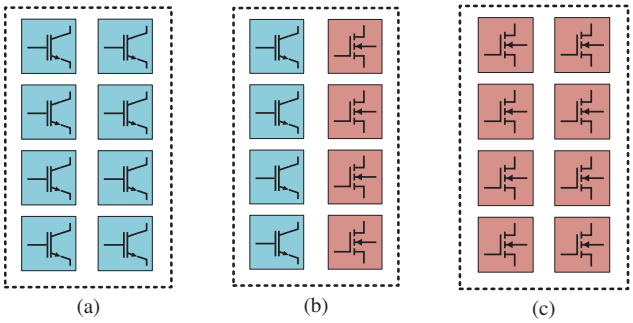

Fig. 4. The three configurations for the inverter switches considered in this study: eight discrete IGBTs with anti-parallel diodes in parallel (a), four discrete IGBTs (no anti-parallel diode) with four discrete MOSFETs in parallel (b), and eight discrete MOSFETs in parallel (c).

TABLE I
NISSAN LEAF DRIVE TRAIN PARAMETERS [25]

Parameter	Value	Unit
Battery DC Voltage	375	V
Battery Capacity	24	kWh
Output Power	80	kW
Switching Frequency	5	kHz

II. SI/SIC HYBRID SWITCH

A. Selection of Devices

HySs are realized by paralleling Si IGBTs and SiC MOSFETs. These semiconductor devices are commercially sold as power modules, as illustrated in Fig. 3 (a) or as discrete TO-packaged devices as shown in Fig. 3 (b). Both packaging configurations of Si IGBT and SiC MOSFET are popular solutions with many different suppliers. Paralleling discrete devices introduces significant parasitic inductances that can negatively affect the commutation loop [9]. In this context, integrating the HyS in a single packaging would reduce parasitic inductance and lead to optimal performances [12]. Due to limited products available commercially, in this study, the HyS is realized paralleling several single switch TO-247 packaged discrete components.

As previously mentioned, the HyS is designed for the implementation in the drive train of the Nissan Leaf 2011 Model, whose main electrical parameters are listed in Table I [25]. Due to the available commercial products and the modularity of the design, the current rating of each HyS has been chosen to be about 300 A.

Three different configurations of the same current rating, based on off-the-shelf components, are compared, and they are displayed in Fig. 4(a)-(c) The full Si IGBT and full SiC MOSFET configurations where eight discrete components are arranged in parallel for each inverter switch are shown in Fig. 4(a) and (c). The HyS-based solution, assembled with four discrete IGBTs in parallel with four discrete SiC MOSFETs per inverter switch, is shown in Fig. 4(b). An 1:1 Si/SiC rated current ratio has been considered in this study to ensure that the switch would operate within the thermal limitation.

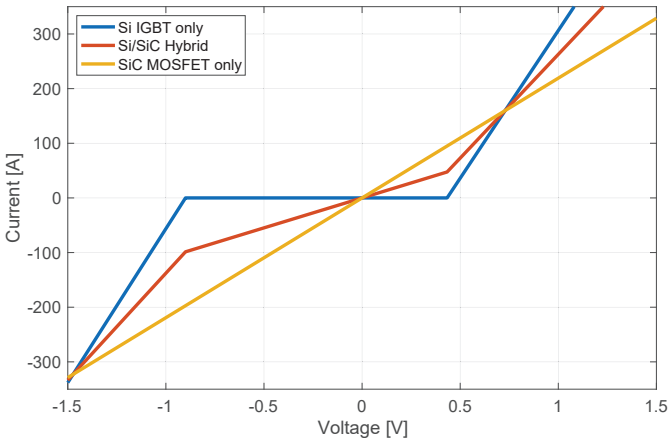

Fig. 5. The on-state characteristics of all three configurations considered in this paper.

Therefore, the SiC MOSFETs and Si IGBTs in the HyS are designed to have equal current rating. The low voltage of the EV battery allows the utilization of switches with 650V voltage class. The specific selection of components and their ratings can be found in Table II. The traction inverter is then designed paralleling two of the previously described switches, so to withstands the total phase current.

B. Switch Characteristics

A linearized model was created in LTSpice based on the data extracted from the manufacturer's datasheet.

The on-state behaviour of the three configurations studied can be observed in Fig. 5. The on-state characteristics are derived for a parallel of eight devices, as it has been previously described. For low current values, between -100 and 100 A, in the HyS, this flows entirely through the SiC MOSFET, however the on-state characteristics differs from the full MOSFET switch, as possible to see in Fig. 5. This difference is due to the fact that the HyS is composed of four parallel MOSFET, while the full MOSFET one by eight parallel devices. Therefore, at low current, the pure SiC MOSFET switch will exhibit half on-state resistance than the HySs.

As predicted, the HyS has a trade-off performance when compared to the single technology configurations. As it can be noted the HyS demonstrate a lower voltage drop at equal forward current than the full Si IGBT switch at low currents and better performance than the full SiC MOSFET switch at high current. The on-state characteristics are compared at 150°C, which is the maximum temperature at which the switches are designed to operate.

C. Current Sharing

The current sharing between the IGBT and MOSFET in the HyS varies according to the total current and temperature. To visualize this, the on-state characteristic is linearized between 0°C and 150°C and swept between -300A to 300A, as shown in Fig. 6 and 7. At low current, the total current flows through the MOSFET due to the IGBT's pn junction barrier voltage.

TABLE II
OFF-THE-SHELF COMPONENTS CONSIDERED FOR THE STUDY [22], [23].

Switch	Producer	Type	Rating	Price [$][1]
SCT3030AL	Rohm	SiC MOSFET	49A / 650V	22.23
IGP40N65H5	Infineon	Si IGBT	46A / 650V	4.29

[1] taken from Digi-Key [24].

When the junction barrier voltage is reached, the IGBT starts to share the total current with the MOSFET. As the current increases, more current flows through the IGBT, as it has a lower on-state resistance than the MOSFET. Similar current sharing behaviour can be observed between the diode of the IGBT and MOSFET in the negative current region.

Due to the intrinsic positive temperature coefficient of the used semiconductor devices, their on-state characteristic is strongly influenced by their junction temperatures. As junction temperature, T_j, increases, the conduction performance deteriorates because the on-state resistance, R_on, increases. The temperature dependence of R_on is linear and can be expressed as:

$$R_\mathrm{on}(T_\mathrm{j}) = R_\mathrm{on,ref} \cdot [1 + C_\mathrm{t} \cdot (T_\mathrm{j} - T_\mathrm{ref})], \quad (1)$$

where C_t is the linear coefficient and $R_\mathrm{on,ref}$ the on-state resistance at the reference temperature T_ref. The SiC MOSFET component has a higher C_t than the Si IGBT, therefore, the IGBT, with its lower on-state resistance, would conduct a higher percentage of the total current at higher junction temperature. Furthermore, the IGBT's junction barrier potential decreases as temperature increases. This means that the IGBT starts conducting current at a lower total current.

III. EFFICIENCY EVALUATION

Power losses in Pulse-Width-Modulation (PWM) controlled three phase Two-Level inverters occurs due to current conduction, P_c, and switching, P_sw:

$$P_\mathrm{losses} = P_\mathrm{c} + P_\mathrm{sw}. \quad (2)$$

These can be calculated based on the assumption that the switching frequency f_s is much greater than the fundamental motor frequency. The EV is assumed to also implement a sinusoidal carrier based PWM, which means the sinusoidal carrier can be considered constant during one switching period. For the full Si IGBT solution the conduction losses are calculated using the on-state resistance, r_ce, and pn barrier voltage, v_ce, as described in the previous section:

$$P_\mathrm{c} = v_\mathrm{ce} \cdot I_\mathrm{avg} + r_\mathrm{ce} \cdot I_\mathrm{rms}^2, \quad (3)$$

where I_rms and I_avg are the RMS and average current flowing through the device. The hard switching losses, instead, are calculated using the turn on, off, and reverse recovery switching energies $E_\mathrm{on,off,rr}(I_\mathrm{sw}(\theta))$, which are function of the switched current $I_\mathrm{sw}(\theta)$. These are provided by the manufacturers in datasheets and can be linearly scaled according to the switched voltage $V_\mathrm{dc,sw}$ and reference voltage V_b given in the datasheet:

$$P_\mathrm{sw,IGBT,MOS} = \frac{f_\mathrm{s} V_\mathrm{dc,sw}}{2\pi V_\mathrm{b}} \int_0^{2\pi} E_\mathrm{on,off,rr}(I_\mathrm{sw}(\theta))\mathrm{d}\theta \quad (4)$$

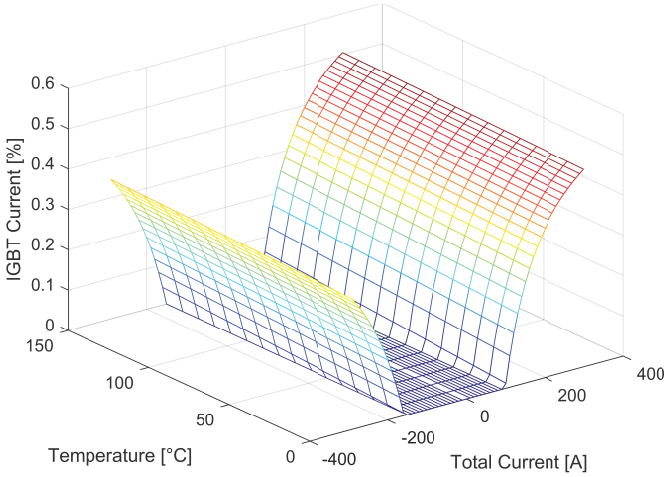

Fig. 6. Percentage of current flowing through IGBTs as a function of the current and temperature for the HyS.

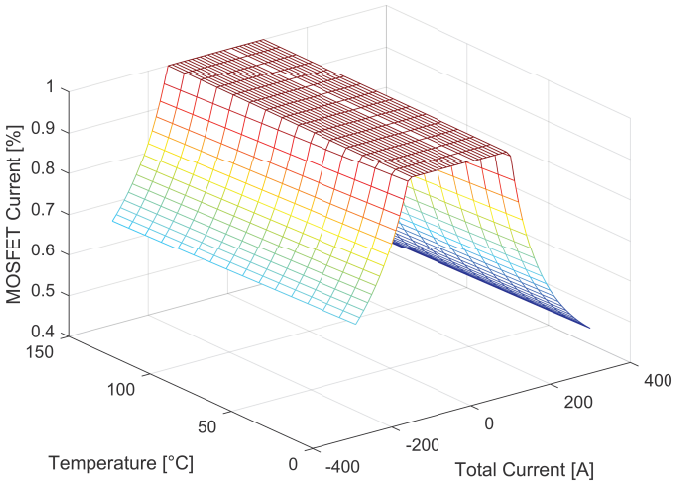

Fig. 7. Percentage of current flowing through MOSFETs as a function of the current and temperature for the HyS.

The average and RMS current flowing through the IGBT and diode of the full Si IGBT inverter are calculated using the (5)-(8), where $\hat{I}$ indicates the peak AC current, m the modulation index, and φ is the phase shift between voltage and current at fundamental frequency:

$$I_{\mathrm{avg,T}} = \frac{\hat{I}}{8\pi}\left(m\pi\cos\varphi + 4\right) \tag{5}$$

$$I_{\mathrm{avg,D}} = \frac{\hat{I}}{8\pi}\left(4 - m\pi\cos\varphi\right) \tag{6}$$

$$I_{\mathrm{rms,T}} = \frac{\hat{I}}{2}\sqrt{\frac{8m\cos\varphi + 3\pi}{6\pi}} \tag{7}$$

$$I_{\mathrm{rms,D}} = \frac{\hat{I}}{2}\sqrt{\frac{3\pi - 8m\cos\varphi}{6\pi}} \tag{8}$$

For the conduction losses of the full SiC MOSFET solution one can use:

$$P_{\mathrm{c}} = r_{\mathrm{dson}} \cdot I^2_{\mathrm{rms,M}} \tag{9}$$

where r_{dson} is the on-state resistance of the MOSFET and the RMS current flowing through it, I_{rms}, is defined as:

$$I_{\mathrm{rms,M}} = \frac{\hat{I}_{\mathrm{ac,MOS}}}{2} \tag{10}$$

assuming that the dead time is relatively small with respect to the switching period and that the current ripple in the motor phases is negligible.

The forward conduction losses of the HySs between IGBT and MOSFET is calculated by integrating the the product of the instantaneous current flowing through the switch $I(\theta)$, the voltage across the switch $V(I(\theta))$, which is the voltage corresponding to the instantaneous current in the on-state characteristic curve, and the duty cycle $D(\theta)$ of the inverter:

$$P_{\mathrm{c}} = \frac{1}{2\pi}\int_{\varphi}^{\pi+\varphi} I(\theta+\varphi)\cdot V(I(\theta))\cdot D(\theta)d\theta, \tag{11}$$

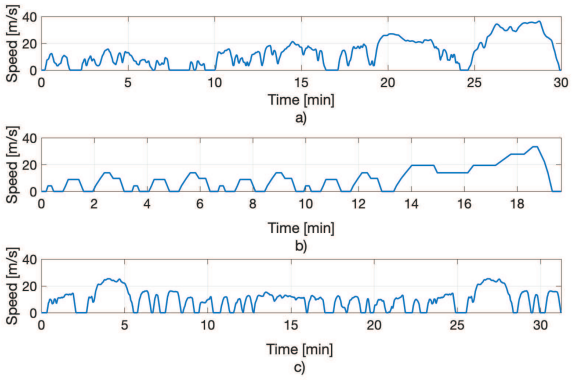

Fig. 8. The speed profiles of a) WLTP, b) NEDC, and c) FTP driving cycle.

where for sinusoidal PWM

$$D(\theta) = \frac{1}{2} + \frac{1}{2}m\sin\theta. \tag{12}$$

The reverse conduction losses of the HySs is given by:

$$P_{\mathrm{c}} = \frac{1}{2\pi}\int_{\varphi}^{\pi+\varphi} I(\theta+\varphi)\cdot V(I(\theta))\cdot (1 - D(\theta))d\theta \tag{13}$$

The equations here described are implemented in MATLAB and used to evaluate the efficiency of the HyS inverter both at static load condition and over standardized driving cycles, displayed in Fig. 8.

A. *Efficiency over Static Load Conditions*

At static load, the efficiency of each switch is evaluated at unit power factor from 10% loading to full load, considering a junction the temperature of 80°C. The modulation index is 0.5 and the switching frequency is 5000Hz, according to the Nissan Leaf traction drive. The inverter efficiency varying the output power is plot in Fig. 9. At low power the MOSFET and HyS-based inverters show significantly better efficiency than the IGBT-based one. As the load increase, the three switch configuration show similar performances.

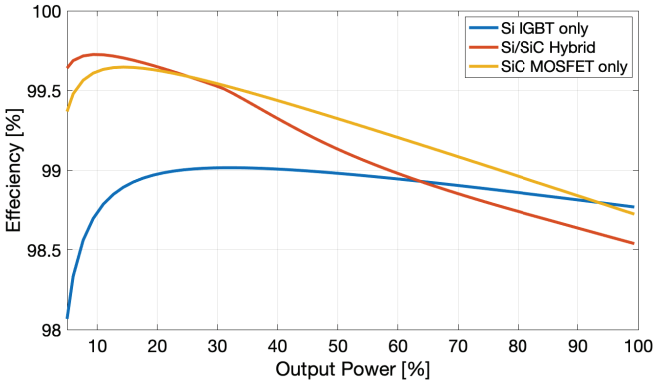

Fig. 9. Efficiencies of all configurations as a function of output power.

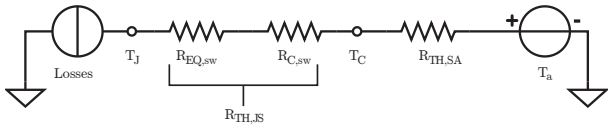

Fig. 10. The simplified thermal circuit for Heatsink design.

B. *Efficiency over Driving Cycle*

To evaluate the efficiency of the inverter for EV, the Nissan Leaf car model is simulated when performing the WLTP, FTP and NEDC driving cycles [26], which are standardized driving cycles used for the benchmarking of transport vehicles, in MATLAB Simulink. Each driving cycle has a duration which varies from 20 to 30 minutes, as it is possible to see in Fig. 8. For the driving simulation, the vehicle is considered to run in a flat surface with zero inclination.

The voltage, current and modulation data is then input into a feedback loop with the thermal circuit to determine the losses of the inverter. In the feedback loop, the on-state characteristics determined by the thermal circuit is used to calculate the losses with (2)-(13). The simplified thermal resistance circuit of the inverter is shown in Fig. 10. To ensure that the vehicle would operate within the thermal limits, a water cooling system is designed for the inverter. The heatsink thermal resistance, $R_{\mathrm{th,sa}}$, varies for each configuration and is determined by:

$$R_{\mathrm{th,sa}} = \frac{T_{\mathrm{j,max}} - T_{\mathrm{a,max}}}{P_{\mathrm{loss}}} - R_{\mathrm{th,js}}, \tag{14}$$

where $T_{\mathrm{a,max}}$ and $T_{\mathrm{j,max}}$ are the maximum ambient and junction temperature set respectively to 75° and 125°C, and $R_{\mathrm{th,js}}$ the junction to sink thermal resistances, from datasheet. The HySs and MOSFET-based inverters require a smaller heatsink than the IGBT-based counterpart, due to the better efficiency at full power, which is advantageous as it reduces the weight and size of the traction drive.

The ideal switching strategy, as shown in Fig. 2(b), can result in lower switching losses. However, the extent of loss reduction depends on the parasitic inductances and capacitances of the switches. These values are highly dependent on the practical implementation of the switch, which is why

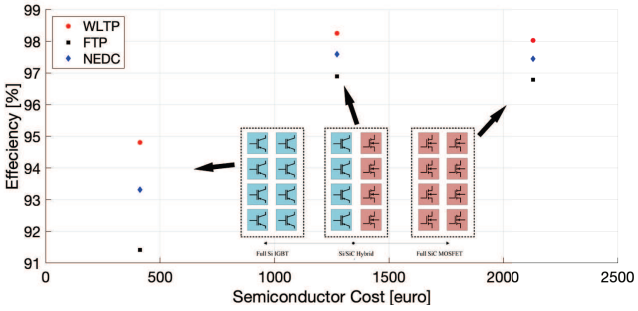

Fig. 11. The efficiency of all configurations over different driving cycles.

the evaluation of efficiency are based on the ideal switching conditions, i.e. the MOSFET takes the turn-on and off losses while the body-diode of the MOSFET takes the reverse recovery losses.

The efficiency of each configuration over the driving cycles and its cost is shown in Fig. 11. The cost figures are derived according to the unit price reported in Table II, and considering that each half-bridge switch of the three phase inverter is assembled paralleling two of switch configurations studied through the paper and displayed in Fig. 4. Each of these, in fact, is rated for conducting 300A, while the phase current when the traction inverter delivers the full power can reach up to 600A.

The driving cycles require the car to be often operating at low partial load. This explains why the solutions employing SiC MOSFETs perform considerably better, especially the ones assembled with the HySs which demonstrate promising overall efficiency. In terms of cost competitiveness, HyS, at the present day component costs, cannot match the low costs of Si IGBTs, however they are considerably cheaper than SiC MOSFETs and show good performances too. Overall, when evaluating efficiency and costs, the HyS is worth to be considered as promising switch candidate for the EV traction application.

IV. Conclusion and Future Work

This paper investigated the performances of hybrid Si/SiC inverters for EV drive trains. Due to the fact that the EVs operate most of the time at low partial load, the IGBT based traction inverter operates at a disadvantage point, since it does not have the best performance at low current. In this merit, the HyS constitutes a superior alternative. It has the advantages of both the Si IGBT and SiC MOSFET, exhibiting a good on-state characteristics over the entire operating range. Furthermore, it has a considerably lower cost than the full SiC MOSFET switch. Although the pure IGBT inverter has higher efficiency near full load, multiple standardized driving cycles suggest that evaluating inverter efficiency at partial load is more important in this specific application, making the HyS a valuable candidate and EV traction inverter switch.

For future studies, the HyS of the selected configuration will be experimentally characterized and compared, so to validate

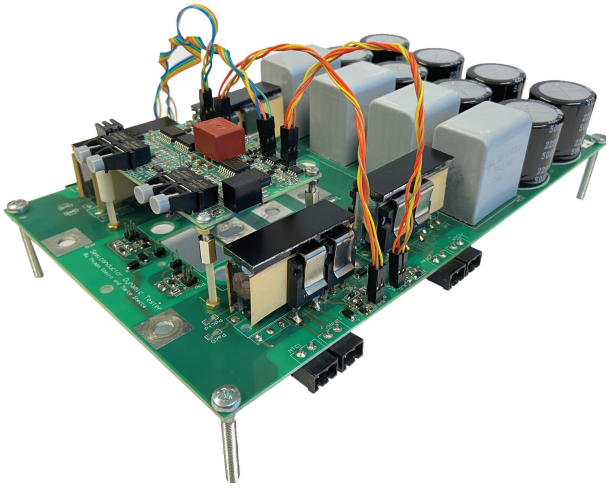

Fig. 12. Test board for the characterization of module and TO-packaged discrete semiconductors.

the models utilized in this paper. The test board designed for the characterization of module and TO-packaged discrete semiconductors, shown in Fig. 12, will be used. The switching strategy, individual component chip size and rated current ratio between Si IGBT and SiC MOSFET should also be examined to further optimize the performances and decrease cost. Furthermore, the efficiency should be experimentally compared with the driving cycle load profile. A Hardware In the Loop implementation would be ideal for this test to prove the advantage of Si/SiC HyS for consumer EVs.

REFERENCES

[1] M. Su, C. Chen, S. Sharma and J. Kikuchi, "Performance and cost considerations for SiC-based HEV traction inverter systems," 2015 IEEE 3rd Workshop on Wide Bandgap Power Devices and Applications (WiPDA), Blacksburg, VA, 2015.

[2] K. Shenai, R. S. Scott, and B. J. Baliga, "Optimum semiconductors for high power electronics," IEEE Trans. Electron Devices, vol. 36, no. 9, pp. 1811–1823, Sep. 1989.

[3] M. Rahimo et al., "Characterization of a silicon IGBT and silicon carbide MOSFET cross-switch hybrid," IEEE Trans. Power Electron., vol. 30, no. 9, Sep. 2015.

[4] G Ortiz, C Gammeter, J W Kolar, et al. "Mixed MOSFET-IGBT bridge for high-efficient medium-frequency dual-active-bridge converter in solid state transformers," 2013 IEEE 14th Workshop on Control and Modeling for Power Electronics (COMPEL). IEEE, 2013.

[5] J. S. Lai et al.,"A hybrid-switch-based soft-switching inverter for ultrahigh-efficiency traction motor drives," IEEE Trans. Ind. Appl., vol. 50, no. 3, May/Jun. 2014.

[6] K. Ishikawa, S. Yukutake, Y. Kono, K. Ogawa and N. Kameshiro, "Traction inverter that applies compact 3.3 kV / 1200 A SiC hybrid module," 2014 International Power Electronics Conference (IPEC-Hiroshima 2014 - ECCE ASIA), Hiroshima, 2014.

[7] J. He, R. Katebi and N. Weise, "A Current-Dependent Switching Strategy for Si/SiC Hybrid Switch-Based Power Converters," in IEEE Transactions on Industrial Electronics, vol. 64, no. 10, Oct. 2017.

[8] R. A. Minamisawa, U. Vemulapati, A. Mihaila, C. Papadopoulos and M. Rahimo, "Current Sharing Behavior in Si IGBT and SiC MOSFET Cross-Switch Hybrid," in IEEE Electron Device Letters, vol. 37, no. 9, Sept. 2016.

[9] A. Deshpande and F. Luo, "Practical Design Considerations for a Si IGBT + SiC MOSFET Hybrid Switch: Parasitic Interconnect Influences, Cost, and Current Ratio Optimization," in IEEE Transactions on Power Electronics, vol. 34, no. 1, Jan. 2019.

[10] Z. Zhang, L. Zhang and J. Qin, "Optimization of Delay Time between Gate Signals for Si/SiC Hybrid Switch," 2018 IEEE Energy Conversion Congress and Exposition (ECCE), Portland, OR, 2018.

[11] H. Cao, P. Ning, T. Yuan and X. Wen, "A 1200V/400 A Hybrid Module with Si-IGBT and SiC-MOSFET Development," PCIM Asia 2019; International Exhibition and Conference for Power Electronics, Intelligent Motion, Renewable Energy and Energy Management, Shanghai, China, 2019.

[12] L. Li, P. Ning, X. Wen and D. Zhang, "A 1200 V/200 a half-bridge power module based on Si IGBT/SiC MOSFET hybrid switch," in CPSS Transactions on Power Electronics and Applications, vol. 3, no. 4, Dec. 2018.

[13] X. Song and A. Q. Huang, "6.5kV FREEDM-Pair: Ideal high power switch capitalizing on Si and SiC," 2015 17th European Conference on Power Electronics and Applications (EPE'15 ECCE-Europe), 2015.

[14] Q. Guan et al., "An Extremely High Efficient Three-Level Active Neutral-Point-Clamped Converter Comprising SiC and Si Hybrid Power Stages," in IEEE Transactions on Power Electronics, Oct. 2018.

[15] S. G. Rosu, M. Khalilian, V. Cirimele and P. Guglielmi, "A dynamic wireless charging system for electric vehicles based on DC/AC converters with SiC MOSFET-IGBT switches and resonant gate-drive," IECON 2016 - 42nd Annual Conference of the IEEE Industrial Electronics Society, Florence, 2016.

[16] A. Deshpande, Y. Chen, B. Narayanasamy, A. S. Sathyanarayanan and F. Luo, "A three-level, T-type, power electronics building block using Si-SiC hybrid switch for high-speed drives," 2018 IEEE Applied Power Electronics Conference and Exposition (APEC), San Antonio, TX, 2018.

[17] "What is the Worldwide Harmonised Light Vehicle Test Procedure?", WLTPfacts.eu, 2020. [Online]. Available: https://www.wltpfacts.eu/what-is-wltp-how-will-it-work/.

[18] A. Semon and A. Crăciunescu, "Study to Increase the Efficiency of the Electric Drive System of a Vehicle at Different Speeds," 2019 11th International Symposium on Advanced Topics in Electrical Engineering (ATEE), Bucharest, Romania, 2019.

[19] P. Ning, L. Li, X. Wen and H. Cao, "A hybrid Si IGBT and SiC MOSFET module development," in CES Transactions on Electrical Machines and Systems, vol. 1, no. 4, pp. 360-366, Dec. 2017.

[20] Cree, "CAS120M12BM2-All-Silicon Carbide Half-Bridge Module," 2014. [Online]. Available: http://www.https://www.wolfspeed.com/

[21] Infineon, "IKW30N65ES5-TRENCHSTOPTM 5 high Speed soft switching IGBT with full current rated RAPID 1 diode," 2015. [Online]. Available: http://www.infineon.com/

[22] Infineon, "Infineon IGBT discrete." [Online]. Available: https://www.infineon.com/cms/en/product/power/igbt/igbt-discretes/.

[23] Rohm Semiconductor, "Rohm Semiconductor SiC Power Devices." [Online]. Available: https://www.rohm.com/products/sic-power-devices.

[24] Digi-Key, "Digi-Key Electronics." [Online]. Available: https://www.digikey.nl/.

[25] R. Yang, "Electrified vehicle traction machine design with manufacturing considerations", Ph.D. thesis, McMaster University, Hamilton, ON, Canada 2016.

[26] A. Kempitiya and W. Chou, "An electro-thermal performance analysis of SiC MOSFET vs Si IGBT and diode automotive traction inverters under various drive cycles," 2018 34th Thermal Measurement, Modeling Management Symposium (SEMI-THERM), San Jose, CA, 2018, pp. 213-217